MODELING GEOMAGNETIC FIELD REVERSALS WITH COUPLED PARTICLES IN A DOUBLE-WELL POTENTIAL

Klaudio PEQINI
Department of Physics, Faculty of Natural Sciences, University of Tirana, Albania
Author for correspondence: klaudio.peqini@fshn.edu.al
KP, 0000-0002-8516-7381

ABSTRACT

We study a minimal model of geomagnetic field reversals, inspired by Molina-Cardin *et al*. (2021), in which two particles evolve in a double-well potential and interact through elastic coupling. One particle evolves slowly, while the other evolves more rapidly, representing distinct dynamical scales of the geodynamo. We explore two formulations of this system: a first-order diffusive (Brownian) version and a second-order inertial (Langevin) version. These formulations exhibit markedly different statistical behaviors: the Brownian model tends to generate unrealistically frequent reversals, especially when calibrated with limited datasets, whereas the Langevin model produces reversal sequences that align more closely with the long-term geomagnetic record. Using two different palaeomagnetic records and comparing the resulting reversal series with several extended polarity timescales, we demonstrate that the model's behavior is highly sensitive to the choice of palaeomagnetic record. While the diffusive version produces an unrealistic number of reversals, the Langevin version shows a qualitative consistency with polarity records. These findings highlight the need for high-quality, long-duration datasets and support the inclusion of inertial dynamics to suppress spurious reversal events. Although the two-particle framework provides insights into the interplay between fast and slow processes in the outer core, its simplicity imposes limitations. We conclude that future developments should aim to extend the model with additional degrees of freedom—potentially through coupling with spatially structured systems—to better capture the complexity of geomagnetic reversals observed in both palaeomagnetic data and numerical geodynamo simulations.

***Keywords*:** dynamo theory, particles and well, palaeomagnetic measurements, asymmetry of reversals, Brownian model

1. INTRODUCTION

The Earth's magnetic field (also known as the geomagnetic field) is one of the most extensively studied magnetic properties of astrophysical objects (Merrill *et al*. 1996). A wealth of direct measurements and historical data exists, covering a wide range of temporal and spatial scales—from thousands to millions of years (Valet and Meynadier, 1993; Guyodo and Valet, 1999; Valet *et al*. 2006; Guyodo and Valet, 2006; Ziegler and Constable, 2011). The field is generated by the geodynamo mechanism, which involves convective flows in the liquid outer core driven by thermal and compositional gradients (Backus *et al*. 1996; Kageyama and Sato, 1997). These flows interact in complex ways with the ambient magnetic field (Dormy and Soward, 2007; Duka *et al*. 2015), giving rise to a highly intricate system. Despite these complexities, the geomagnetic field is predominantly dipolar in nature (Merrill *et al*. 1996; Backus *et al*. 1996; Duka *et al*. 2015; Peqini *et al*. 2015), resembling the field of a giant bar magnet tilted approximately 11 degrees from the Earth's rotational axis. However, unlike a simple bar magnet, this field is not stable: it has reversed polarity numerous times throughout geological history.

Over geological timescales, polarity reversals—during which the magnetic North and South poles switch places—occur irregularly. The interval between successive reversals ranges from hundreds of thousands to several million years, representing some of the longest-timescale variations observed in the geomagnetic record (Backus *et al*. 1996). On average, reversals occur every 200,000 to 300,000 years, although the frequency has varied significantly over time (Valet and Meynadier, 1993; Backus *et al*. 1996; Guyodo and Valet, 2006; Olson *et al*. 2010; Mori *et al*. 2013; Duka *et al*. 2015; Peqini *et al*. 2015; Valet and Fournier, 2016). These fluctuations in reversal rates are striking (see Fig. 1), with intervals of frequent reversals alternating with superchrons—extended periods, such as the Cretaceous Normal Superchron, which lasted up to 38 million years with virtually no reversals (Cande and Kent, 1992).

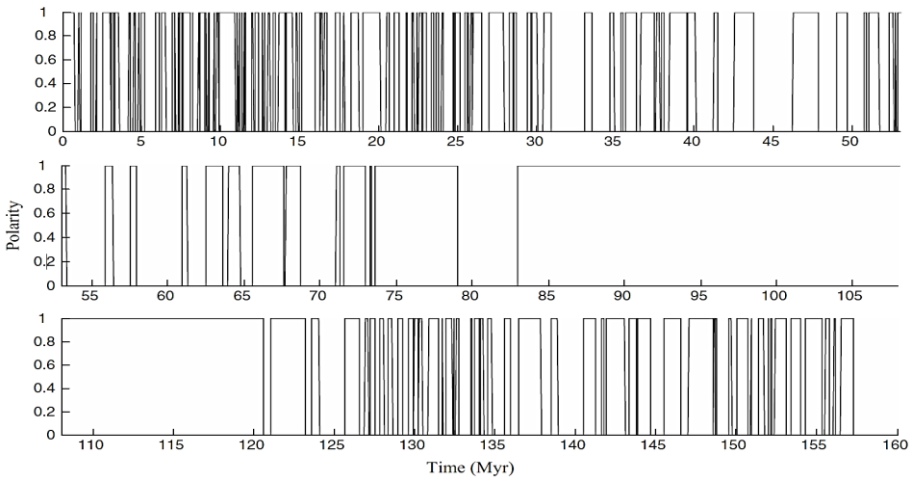

Fig. 1: The time series of the polarity reversals for the period of 157.5 Myr provided by Cande and Kent (1992). There it is shown the polarity of the Dipolar field for the last 157.5 million years. The time "0" refers to the present (adapted from Duka *et al.* 2015).

In recent years, low-dimensional geomagnetic models—simplified representations of the geodynamo—have received increasing attention in the scientific literature (Mori *et al.* 2013; Duka *et al.* 2015; Peqini *et al.* 2015; Molina-Cardin *et al.* 2021; Peqini, 2024). Rather than attempting to reproduce the full complexity of the geodynamo, these models focus on specific aspects of geomagnetic behavior, such as dipolar field reversals. The aim is to extract meaningful insights from an inherently complex system governed by intricate dynamical equations. Despite their simplicity, these models have proven successful in providing coherent explanations for key features of geomagnetic reversals. For example, they offer insight into the mechanisms underlying polarity switches (Mori *et al.* 2013; Duka *et al.* 2015) and explain the intermittent nature of reversals, often attributed to the intrinsic stochasticity of the system (Duka *et al.* 2015; Peqini *et al.* 2015; Molina-Cardin *et al.* 2021).

One low-dimensional model has successfully reproduced a key feature of the geomagnetic reversal mechanism: the slow decay of the dipolar field followed by its rapid recovery with opposite polarity (Molina-Cardin *et al.* 2021). This asymmetry is well documented in palaeomagnetic time series (Valet and Meynadier, 1993; Guyodo and Valet, 1999; Valet *et al.* 2005; Guyodo and Valet, 2006; Ziegler and Constable, 2011). In this

paper, we examine two existing versions of this model and assess whether they can account for additional observed patterns of geomagnetic reversals. Although low-dimensional models inherently possess limited scope, they nevertheless provide opportunities for further development to more accurately capture the underlying system. In this work, we explore such extensions and evaluate their potential to enhance the model's explanatory power.

The paper is organized as follows: in Section 2, we describe the model proposed by Molina-Cardín *et al.* (2021). Section 3 presents key results, while Section 4 discusses additional aspects of the model, including its strengths and limitations. This section also introduces several proposed modifications and extensions aimed at improving the model's performance. Finally, Section 5 offers concluding remarks and outlines potential directions for future research.

2. Particles in a well model

The *particles-in-a-well* model represents an interesting and relatively simple low-dimensional framework (see Fig. 1 in Molina-Cardín *et al.* 2021). Two versions of this model can be constructed: the diffusive version, as introduced by Molina-Cardín *et al*. (2021), and a second-order version derived from Langevin-type dynamical equations (Peqini, 2024).

An earlier and relatively successful model was that of a single particle in a double-well potential (Schmitt *et al*., 2001). In this model, the particle undergoes Brownian motion within a quartic potential of the form:

$$V(x) = ax^4 + bx^2 + c$$

Here the particle's position represents the magnitude of the dipolar geomagnetic moment, while its Brownian motion reflects the random-like temporal variations observed across multiple timescales (Merrill *et al*. 1996; Schmitt *et al*. 2001; Aubert *et al*. 2013; Buffett *et al*. 2013; Morzfeld and Buffett, 2019). Each minimum of the potential—i.e., each well—corresponds to a stable configuration of the dipolar magnetic field: the positive well represents the normal polarity state, and the negative well represents the reversed polarity state. Within this framework, geomagnetic reversals are interpreted as intermittent transitions of the particle between wells. However, although this model provides a compelling statistical interpretation of reversals, the inherent symmetry of the potential prevents

it from capturing the observed asymmetry between the slow decay and rapid recovery phases of real geomagnetic reversals.

Before presenting the mathematical formulation of the model, it is helpful to clarify the motivation underlying the particles-in-a-well framework. The two-particle approach adopted here extends a long-standing tradition of reducing the complex geodynamo dynamics into low-dimensional systems that capture essential features of geomagnetic polarity reversals. Gubbins (1988), for instance, suggested that reversals may arise from interactions between two competing dynamo modes: a dominant axial dipole and a secondary non-axisymmetric mode that can destabilize the system under certain conditions. This dual-mechanism perspective provides the conceptual foundation for our two-particle representation. In this analogy, one particle corresponds to the slow evolution of the dominant dipolar component, while the other represents faster, potentially destabilizing fluctuations associated with higher-order modes or turbulence. The elastic coupling between the two particles introduces dynamic feedback: perturbations in the fast mode can affect the stability of the slow mode, and vice versa. This interplay is essential for reversal dynamics, as it provides a mechanism through which internal fluctuations can trigger large-scale polarity switches.

Further theoretical support for this analogy comes from the distinction between geomagnetic excursions and full reversals, as articulated by Gubbins (1999). In that framework, excursions are interpreted as failed reversals—events potentially triggered by the same underlying mechanism but lacking sufficient perturbation amplitude or duration to fully destabilize the dipolar field. Our model is consistent with this view: depending on the strength and timing of stochastic forcing, the fast particle may either succeed or fail in driving the system across the potential barrier, leading to full reversals or limited excursions. This formulation enables a unified interpretation of both phenomena within a single stochastic system, where the transition probability is governed by the interplay of noise intensity, potential well asymmetry, and coupling strength.

Hoyng *et al*. (2002) further advanced the dual-mode approach by analyzing the statistical variability of the geomagnetic dipole in terms of nonlinear interactions between a stable dipolar mode and a more erratic secondary mode. Their results support the view that reversals are not purely random events but emerge from the interaction of modes with different symmetries and timescales. Our model reflects this structure by assigning distinct dynamical roles to each particle: one with slow,

overdamped dynamics representing the stable dipole, and the other with faster, potentially inertial behavior that introduces irregular forcing. This separation of timescales and roles reinforces the idea that reversals are emergent phenomena driven by internal dynamical coupling rather than externally triggered or purely stochastic processes. By incorporating both diffusive and Langevin formulations, our study further explores how different physical assumptions about the fast mode shape the statistical properties of the resulting reversal sequences.

In this contribution, we restrict our focus to the model's ability to qualitatively reproduce the reversal features reported in the literature. A subsequent paper will provide a more detailed quantitative analysis, with particular emphasis on measures used to characterize reversal asymmetry.

An elegant solution to the asymmetry problem was proposed by Molina-Cardín *et al*. (2021), who extended the earlier single-particle framework by introducing a second particle into the double-well potential, coupled to the first via a spring. Both particles undergo random motion but with different kinetic energies—effectively, distinct "temperatures." The fast particle represents short-term, high-frequency geomagnetic variability, such as secular variation and smaller-scale fluctuations (Guyodo and Valet, 1999; Aubert *et al*. 2013; Morzfeld and Buffett, 2019). By contrast, the slow particle captures long-term variations spanning geological timescales (Backus *et al*. 1996; Merrill *et al*. 1996; Valet *et al*. 2006; Ziegler and Constable, 2011; Wicht and Meduri, 2016). These two classes of timescales are not independent; rather, long-term behavior can be interpreted as a natural consequence of short-term dynamics (Backus *et al*. 1996; Duka *et al*. 2015). The coupling between particles is modeled through an elastic interaction, represented by a spring potential—hence the name of the model. Graphical illustrations and further technical details are provided in Molina-Cardín *et al*. (2021).

The physical and observational motivations discussed above lead to the following Lagrangian:

$$L = \frac{1}{2}\left[\left(\frac{dx_1}{dt}\right)^2 + \left(\frac{dx_2}{dt}\right)^2\right] - \frac{1}{2}K\left(x_2 - x_1\right)^2 - V\left(x_1, x_2\right) \tag{1}$$

Here, the kinetic energy terms correspond to the two particles, each assumed to have unit mass. The elastic term models their interaction through a spring with stiffness constant *K*, while the potential energy term

$V(x_1, x_2)$ defines the double-well structure experienced by each particle. The gradient of this potential determines the force acting on the particles within the well. The system's dynamics are described by a set of Langevin-type equations, expressed as follows:

$$\frac{d}{dt}\left(\frac{\partial L}{\partial\left(dx_i/dt\right)}\right)=\frac{\partial L}{\partial x_i}-\gamma_i\frac{dx_i}{dt}+\sqrt{2k_BT_i\gamma_i}\chi_i,\quad i=1,2 \tag{2}$$

where the γ coefficients represent the drag experienced by each particle, and T_i denotes the temperature associated with each particle. In this context, a higher temperature corresponds to a faster particle. The random variable χ is drawn from the normal distribution with zero mean and unit variance. Following the same steps as in the previous section leads to the Langevin-type version:

$$\begin{cases}\dfrac{d^2x_1}{dt^2}=-\left.\dfrac{dV}{dx}\right|_{x_1}-\gamma_1\dfrac{dx_1}{dt}+K\left(x_2-x_1\right)+\sqrt{2k_BT_1\gamma_1}\chi_1\left(t\right)\\ \dfrac{d^2x_2}{dt^2}=-\left.\dfrac{dV}{dx}\right|_{x_2}-\gamma_2\dfrac{dx_2}{dt}+K\left(x_1-x_2\right)+\sqrt{2k_BT_2\gamma_2}\chi_2\left(t\right)\end{cases} \tag{3}$$

The diffusive model, obtained by neglecting the second time derivative, is given by:

$$\begin{cases}\dfrac{dx_1}{dt}=\dfrac{1}{\gamma_1}\left[-\left.\dfrac{dV}{dx}\right|_{x_1}+K\left(x_2-x_1\right)+\sqrt{2k_BT_1\gamma_1}\chi_1\left(t\right)\right]\\ \dfrac{dx_1}{dt}=\dfrac{1}{\gamma_2}\left[-\left.\dfrac{dV}{dx}\right|_{x_2}+K\left(x_1-x_2\right)+\sqrt{2k_BT_2\gamma_2}\chi_2\left(t\right)\right]\end{cases} \tag{4}$$

In both cases of V', indicates the partial derivative of the potential with respect to the corresponding variable. The variables x_1 and x_2 represent the contributions of the slow and fast particle, respectively, to the total dipolar moment X, also referred to here as the *axial component*. The output of the model is the axial component, $X(t)$, is calculated as below:

$$X(t) = wx_1(t) + (1-w)x_2(t) \quad (5)$$

The weight (w) factor indicates which particle contributes more to the output. For a consistent model, *w* must be less than 0.5, this ensuring that the slow particle predominantly determines the long-term the trend.

The potential function *V*(x), which represents the double-well structure, is obtained by fitting a quartic equation in *x* to the probability density function (PDF) derived from palaeomagnetic dipolar field datasets. These datasets record the geomagnetic dipolar field across geological periods ranging from thousands to millions of years (Valet and Meynadier, 1993; Guyodo and Valet, 1999; Valet *et al*. 2005; Guyodo and Valet, 2006; Ziegler and Constable, 2011). In the study by Molina-Cardín *et al*. (2021), palaeomagnetic records covering the last 800,000 years were used (Guyodo and Valet, 1999).

3. RESULTS

A typical realization of system (3) is shown in Fig. 2. The numerical implementation employs the fourth-order Runge–Kutta method, as discussed in Peqini (2024), which is equally applicable in this context. The fast particle, being at a higher temperature, experiences stronger fluctuations and frequently transitions from one potential well to the other, i.e., the fast component undergoes frequent reversals (red line in Fig. 2). In contrast, the slow particle, owing to its greater inertia, requires substantially more energy to cross between wells (blue line in Fig. 2). As a result, it often pulls the fast particle back to the original well, thereby restoring the initial polarity (as reflected in the similarity between the blue and black lines). A successful reversal of the axial component occurs only when both particles simultaneously approach the threshold of transition to the opposite well. This behaviour arises because the slow particle contributes most to the total axial component, as described by equation (5). Consequently, the model suggests that, prior to a reversal, both particles must drift toward the transition threshold—a process that takes time and reproduces the slow decay phase documented in palaeomagnetic records. Once the reversal occurs, both particles rapidly move toward the minimum of the opposite well. This swift transition reflects the fast recovery phase typically observed after a full dipolar field reversal. In this framework, reversal asymmetry emerges naturally from the elastic interaction between

the slow and fast particles. This feature is robust across numerous simulations and is not merely a statistical anomaly (see Fig. 3, panels E and F, in Molina-Cardín *et al*. 2021).

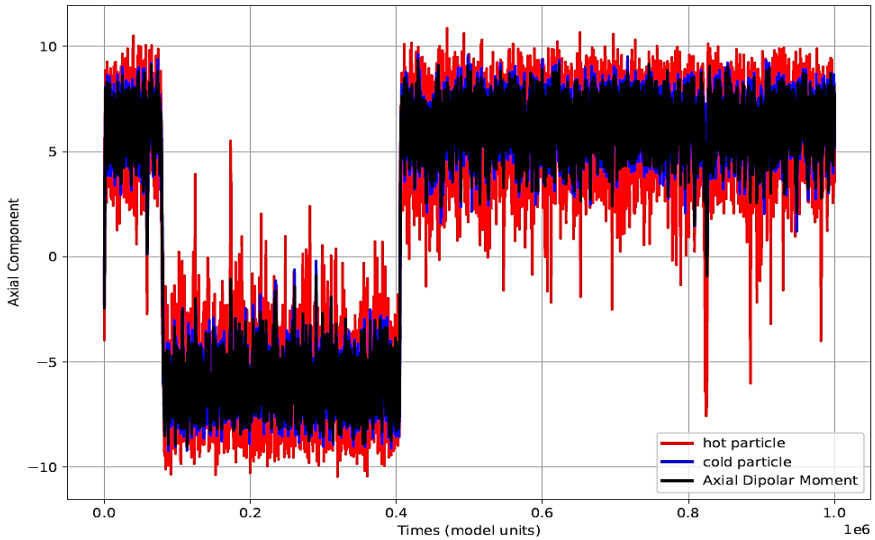

Fig. 2 Typical time series generated by the diffusive particles-in-a-well model (4). The x-axis is expressed in arbitrary time units determined by the characteristic scales of the variables involved in equations (3) and (4). The y-axis represents the axial component of the magnetic dipole, which is not constrained to absolute values of the Geomagnetic Dipole Moment. The term “hot particle” is used interchangeably with “fast particle,” and “cold particle” with “slow particle.” These terms are retained in the legend to allow readers to readily identify the analogous plots presented by Molina-Cardín *et al*. (2021). The axial component is calculated according to equation (5) with $w = 0.2$.

A very similar time series is generated by model (4) as well (plot not shown). However, a comparison of the probability density functions (PDFs) produced by models (3) and (4) reveals notable differences, particularly at the margins (see Fig. 3). These differences indicate that the models capture distinct behaviors during both low- and high-intensity periods—low-intensity phases typically occurring prior to and during reversals, and high-intensity phases characterizing stable epochs. Model (4), the diffusive model, tends to exhibit more frequent reversals and extended periods of stability. This suggests that the decay phase leading up to a reversal is longer, allowing the field to remain in a low-intensity

state for a greater duration. Conversely, the recovery phase following a reversal is much sharper, marked by a rapid transition to a high-intensity state. This interpretation is further supported by the dips observed around the values 5.0 and 15.0 in the PDF. Moreover, the central peak indicates that geomagnetic excursions are more frequent in model (4), likely due to the faster dynamics of the fast particle. In summary, compared to model (3), model (4) is characterized by slower decay, faster recovery, and a higher frequency of excursions.

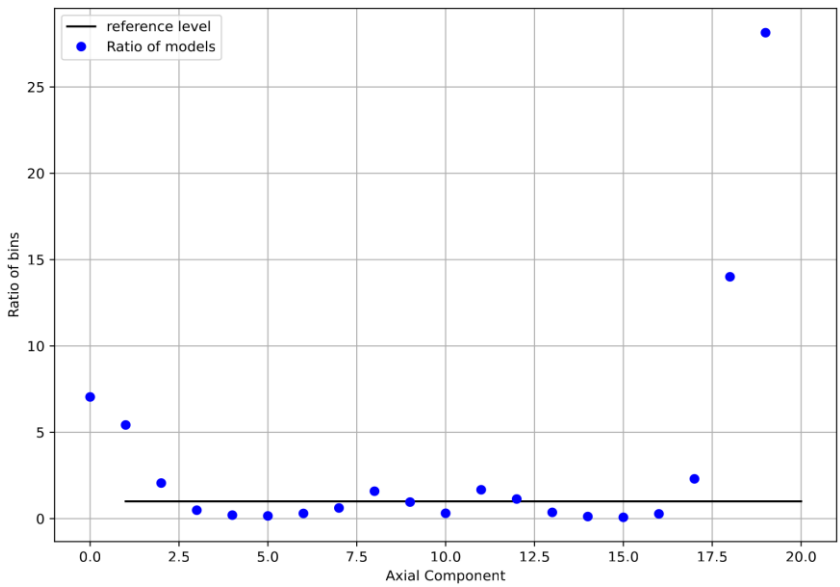

Fig. 3. Ratio plot of the PDFs of the Particles-in-well models (4) and (3). The horizontal line at 1 represents the case where the ratio of the corresponding bins is equal. In this plot, the PDF is divided into 20 bins, which should not be interpreted as absolute values of the axial component of the Dipole Moment. Increasing the resolution to 50 bins does not produce any noticeable qualitative changes, suggesting that the observed differences between the models are essential and robust.

A rather concerning issue arises when comparing the reversal patterns produced by the models with observational data. Figure 4 illustrates the reversal sequences generated by models (3) and (4), respectively. Both models produce polarity intervals of varying lengths; however, model (3) tends to yield longer intervals of stable polarity, indicating less frequent

reversals. This observation helps explain the differences seen in the right-hand bins of the ratio plot in Fig. 3, which reflect reversal statistics. Nevertheless, the total number of reversals generated in these simulations remains relatively low, even after extending the runs beyond 10^6 model time units. The limited reversal count prevents us from drawing firm conclusions as to whether either model (3) or model (4) qualitatively reproduces the reversal frequency observed in the palaeomagnetic record (cf. Fig. 1).

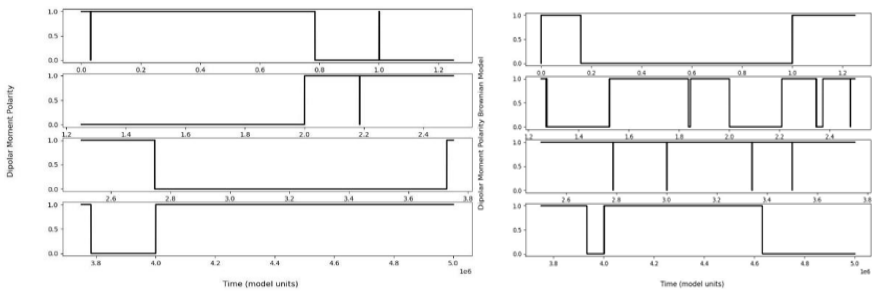

Fig. 4. Reversal patterns generated by the Langevin-type model (3) (left panel) and the Diffusive model (4) (right panel). The *y*-axis indicates the polarity of the dipolar field rather than its magnitude. For clarity, the left panel labels the *y*-axis as "Dipolar Moment Polarity," while the right panel labels it as "Dipolar Moment Polarity (Brownian Model)."

One might suspect that the small number of reversals is not due to insufficiently long simulations. The coefficients of the potential $V(x)$, as employed by Molina-Cardin *et al.* (2021), are $a = 0.00179$ and $b = -0.149$. Furthermore, these authors used a record of the last 800 kyr (Guyodo and Valet, 1999), which contains only one reversal—the Brunhes–Matuyama reversal. In contrast, here we use another record, namely the 4 Myr relative palaeointensity record of Valet and Meynadier (1993) which spans several reversals. The respective coefficients are: $a = 3.188$ and $b = -7.241$ To increase the probability of reversals, the magnitude of each random term in equations (3) or (4) must be significantly higher than that employed by Molina-Cardín *et al*. (2021). A typical simulation of the model with the new parameters yields an (unconstrained) axial component time series qualitatively similar to that shown in Fig. 2 (and is therefore not reproduced here). The change of coefficients does not alter the characteristic dynamics of the system. However, the situation differs

regarding the ratio plot of the two models (3) and (4). As shown in Fig. 5, model (4) dominates in the low and high magnitudes, whilst model (3) dominates in the middle region of the distribution (dominates in the sense that the ratio is large in the boundaries and quite small in the middle). This dependence indicates model (4) produces longer stable periods associated with strong dipolar field, whereas model (3) does not produce a typical dipole-dominated field. The domination of model (4) in the low end of the distribution (associated with very weak dipolar field that is typically observed during reversals) indicates that the particles in the diffusive model are so prone to reversals, as it is corroborated by the right panel in Fig. 6.

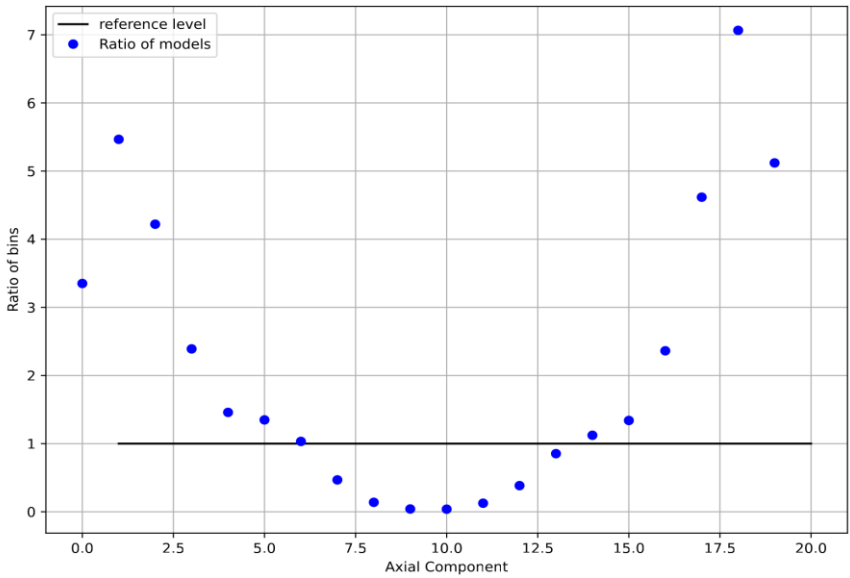

Fig. 5. Ratio plot of the PDFs of the particles-in-wells models (4) and (3), with coefficients determined from the 4 Myr record of Valet and Meynadier (1993). The horizontal line at value 1 corresponds to equal bin ratios. The PDF is constructed with 20 bins, which should not be interpreted as direct values of the axial component of the Dipole Moment. Increasing the number of bins to 50 produces no noticeable qualitative changes, reinforcing that the observed differences between the models are essential rather than numerical artifacts.

The ratio plot reveals that model (4) dominates at the edges of the axial component distribution, whereas model (3) dominates in the central bins. This indicates that model (4) spends more time in states

corresponding to strong dipolar configurations—i.e., near stable polarity states—while model (3) exhibits a higher probability density near the center, corresponding to low dipole amplitudes typically associated with transitional states such as reversals or excursions. Consequently, model (3) appears more prone to generating frequent or prolonged excursions and reversals, reflecting a more dynamic or less stable magnetic regime. By contrast, model (4) favors long-term stability in the axial dipole, with fewer and potentially sharper transitions between polarity states. These distinct occupancy patterns across the axial component range highlight fundamental differences in reversal dynamics between the two models, which may be traced back to differences in damping, inertia, and stochastic forcing structures.

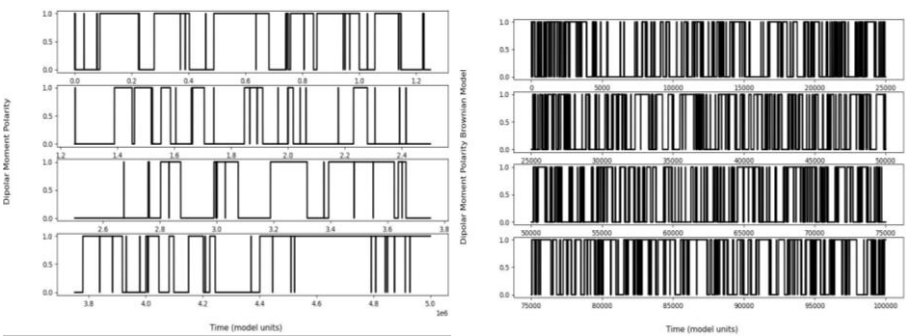

Fig. 6. Reversal patterns generated by the Langevin-type model (3) (left) and the diffusive model (4) (right), using coefficients estimated from the 4 Myr record of Valet and Meynadier (1993). The *y*-axis indicates polarity, not the magnitude of the dipolar field. In the left panel, the axis is labeled "Dipolar Moment Polarity"; in the right panel, "Dipolar Moment Polarity Brownian Model."

The polarity plots obtained by fitting the model coefficients to geomagnetic time series that include multiple reversals highlight the sensitivity of the particle-in-a-well framework to the particular record employed. For example, when applied to the classical Cande and Kent (1992) polarity timescale, the diffusive model generates an unrealistically high frequency of rapid reversals—an artifact inconsistent with paleomagnetic observations (Cande and Kent, 1992; 1995). In contrast, the Langevin (second-order) variant produces reversal sequences that align more closely with the rock record: the spacing, clustering, and occurrence of extended "quiet" intervals between reversals resemble empirical patterns with greater fidelity. Although the present study illustrates results

primarily from the Cande and Kent (1992) dataset, we have repeated the analysis using extended and updated datasets, including the Cande and Kent (1995) timescale, updated Geomagnetic Polarity Timescale (GPTS) compilations for the Cenozoic and Neogene, and sedimentary/igneous records calibrated with10/Be and paleointensity reconstructions (Singer *et al*. 2019). In all cases, the qualitative outcome remains consistent: the diffusive model systematically overproduces rapid reversals, while the Langevin formulation yields reversal sequences with clustering and temporal structure that are more realistic. Supplemental figures are omitted here, but a full quantitative comparison will be presented in a forthcoming publication.

4. DISCUSSIONS

The particles-in-a-well model, though simplified and heuristic, remains a valuable framework for capturing key statistical features of geomagnetic dipole reversals—particularly the asymmetry between decay and recovery phases. Nevertheless, recent analyses demonstrate that the model's behavior is highly sensitive to the choice of palaeomagnetic record used to construct the underlying potential $V(x)$. Earlier formulations, based on the Brunhes–Matuyama reversal recorded over the past 800 kyr (Guyodo and Valet, 1999; 2006), provided limited temporal coverage, encompassing only a single reversal event. To overcome this limitation, we employ more extensive datasets, such as the 4 Myr record of Valet and Meynadier (1993), which captures multiple reversal events. This extended record reflects essential long-term geomagnetic behavior, including intervals of both high and low intensity. However, while it improves the statistical robustness of the model, it does not fully account for very long timescales spanning tens of millions of years, which remain beyond the scope of the present analysis.

Crucially, our findings demonstrate that models derived from extended records behave differently: while the diffusive model tends to overproduce reversals in rapid succession, the Langevin model generates polarity evolutions that more closely match the empirical record. This reinforces earlier arguments (Valet and Meynadier, 1993; Valet *et al*. 2005) regarding the necessity of comprehensive reversal datasets for accurately modelling geomagnetic behaviour. A broader temporal dataset not only enhances the model's capacity to reproduce diverse geodynamo regimes but also improves its statistical robustness, reducing uncertainty

and allowing for more reliable differentiation between genuine geomagnetic signals and random noise (Backus *et al.* 1996; Olson *et al.* 2010). Moreover, the inclusion of extended records increases the likelihood of capturing rare but significant geomagnetic phenomena, such as excursions. Nevertheless, as highlighted by McMillan and Constable (2006) and Panovska *et al*. (2015), the use of older palaeomagnetic records must be approached with caution due to potential issues of temporal resolution, data quality, and post-depositional alteration. Rigorous calibration and cross-validation remain essential before such datasets can reliably inform model construction and interpretation.

The fast and slow particles in the model serve as conceptual proxies for distinct dynamical components of the geomagnetic field, each evolving on characteristic timescales. While these particles do not correspond directly to specific physical structures in the Earth's outer core, their behaviour reflects mechanisms identified in high-fidelity geodynamo simulations. It is well established that the geodynamo operates across a broad spectrum of temporal and spatial scales, driven by turbulent convection in the electrically conducting outer core and modulated by interactions with the solid inner core and mantle (Hollerbach and Jones, 1993; Hollerbach and Jones, 1995; Backus *et al*. 1996; Davidson, 2013). In this context, the slow particle may be interpreted as representing the long-term evolution of the axial dipole field, which numerical simulations demonstrate is stabilized by large-scale, columnar convection aligned with the rotation axis (Aubert *et al*. 2017). These simulations—particularly in the asymptotic rapidly rotating regime—highlight quasi-geostrophic flows that maintain a persistent dipole-dominated magnetic field, analogous to the slowly evolving component captured by the inertial particle.

Conversely, the fast particle may be understood as representing more transient, localized, or non-dipolar contributions to the field, driven by rapidly fluctuating small-scale convection or episodic interactions between convective upwellings and magnetic structures. These processes, observed in simulations, can induce short-term variability and, under certain conditions, trigger reversals (Dormy and Soward, 2007). In addition, mantle control on core dynamics—through thermal anomalies or compositional heterogeneities at the core–mantle boundary—can impose long-wavelength, low-frequency forcing that modulates reversal frequency and stability, including the occurrence of superchrons (Olson and Amit, 2014). While the low-dimensional model does not resolve such spatial structures explicitly, its effective separation into slow and fast

modes reflects this multiscale architecture. Thus, the two-particle system can be viewed as a minimal representation of the competing influences within the dynamo: one stabilizing and long-lived, the other destabilizing and reactive, together shaping the reversal statistics observed in both simulations and the palaeomagnetic record.

The mechanism of geomagnetic reversals in the particles-in-a-well model hinges on the elastic interaction between the two particles, represented by the coupling spring. We suspect that this elastic interaction is a key element of the reversal process. Specifically, the coupling may serve as a mechanism for the gradual accumulation of energy, producing the slow decay phase, followed by a rapid release during the recovery phase after a reversal. This dynamic mirrors the asymmetry observed in geomagnetic reversals. We propose that elastic interactions offer a useful conceptual framework for studying energy transfer processes within the geodynamo. By modeling how energy is stored and subsequently released, these interactions could help illuminate the physical mechanisms underlying geomagnetic field reversals.

5. CONCLUSIONS

The particles-in-a-well model provides a minimal yet insightful framework for exploring the statistical and dynamical features of geomagnetic field reversals. Within this model, reversals are interpreted as stochastic transitions between two stable states of the magnetic dipole, triggered by fluctuations strong enough to overcome an energy barrier. This approach successfully reproduces key observational features of the reversal process, particularly its intermittent nature—characterized by long periods of stable polarity punctuated by rapid transitions—as well as the asymmetry often observed between the decay and recovery phases of the dipole field. A central component of the model's success lies in the inclusion of an elastic coupling between two particles evolving on different timescales, which facilitates energy exchange and controls the reversal dynamics in a physically interpretable manner.

In this study, we have shown that the diffusive and Langevin versions of the model yield markedly different statistical behaviors. When calibrated against extended geomagnetic polarity timescales (Cande and Kent, 1992; Cande and Kent, 1995; Singer *et al*. 2019), the Langevin model proves more consistent with palaeomagnetic observations, avoiding the unrealistic clustering of reversals seen in the diffusive version. This

finding highlights the importance of incorporating second-order dynamics to realistically suppress spurious reversal events and better reflect the stability observed in the long-term geomagnetic record. Moreover, the model's sensitivity to the choice of input dataset underscores the need for using high-quality, well-resolved reversal records when constructing effective potential functions.

Despite these promising features, the two-particle system remains a highly simplified abstraction of the geodynamo. Reducing the complex, multiscale dynamics of Earth's outer core to only two degrees of freedom inevitably limits the model's ability to capture the full range of geomagnetic behavior, particularly when it comes to rare events such as excursions, superchrons, or the influence of mantle heterogeneities. Building on the idea of elastic interactions between dynamical modes, future work will explore their incorporation into more elaborate frameworks, such as the domino model (Duka *et al*. 2015; Peqini *et al*. 2015; Peqini, 2024), which offers greater potential for capturing the spatial and temporal richness of the Earth's magnetic field. This next step aims to bridge the gap between low-dimensional models and fully 3D geodynamo simulations, providing a more comprehensive yet computationally tractable description of geomagnetic reversals.

ACKNOWLEDGEMENTS

We gratefully acknowledge the use of the HPC Cluster acquired through the project *Ngritja e një qendre llogaritëse në mbështetje të bashkëpunimit të IAL-ve shqiptare me projektin europian Compact Muon Solenoid (CMS) në CERN*, funded by AKKSHI. The authors declare no competing interests related to the content of this paper. Further information regarding the algorithms and codes can be found in Peqini *et al*. (2015), where the codes developed for another model can be readily adapted for the particles-in-a-well framework. For additional technical details, interested readers are encouraged to contact the corresponding author directly.

Data accessibility:

There are no databases to be made public, but the codes are available upon request to the author.

Declaration of AI use: There has been no use of AI when writing the actual paper.

Authors' contributions:

K.P.: conceptualization, writing—original draft; validation, writing—review and editing.

All authors gave final approval for publication and agreed to be held accountable for the work performed therein.

Conflict of interest declaration: The author declares there are no conflicts of interest.

Funding: The author declares no funding was received when writing this paper.

REFERENCES

Aubert J, Finlay CC, Fournier A. 2013. Bottom-up control of geomagnetic secular variation by the Earth's inner core. *Nature,* **502 (7470):** 219–223. PMID: 24108054. DOI: 10.1038/nature12574.

Aubert J, Gastine T, Fournier A. 2017. Spherical convective dynamos in the rapidly rotating asymptotic regime. *Journal of Fluid Mechanics*, **813**, 558–593. DOI:10.1017/jfm.2016.789.

Backus G, Constable C, Parker R. 1996. *Foundations of Geomagnetism*. New York, NY: Cambridge University Press.

Buffett BA, Ziegler L, Constable CG. 2013. A stochastic model for palaeomagnetic field variations. *Geophysics Journal International***, 195: 86–97.** doi: 10.1093/gji/ggt218.

Cande SC, Kent DV. 1992. A new geomagnetic polarity time scale for the late Cretaceous and Cenozoic. *Journal of Geophysical Research*, **97 (B10):** 13917–13951. https://doi.org/10.1029/92JB01202.

Cande SC, Kent DV. 1995. Revised calibration of the geomagnetic polarity timescale for the Late Cretaceous and Cenozoic. *Journal of Geophysical Research*, **100 (B4):** 6093–6095. https://doi.org/10.1029/94JB03098.

Constable C, Morzfeld M. 2025. Weather at the core: defining and categorizing geomagnetic excursions and reversals. *Geophysical Journal International*, **240 (1):** 747–762**.** https://doi.org/10.1093/gji/ggae415.

Davidson PA, 2013a. Scaling laws for planetary dynamos. *Geophysical Journal International*, **195 (1):** 67-74. https://doi.org/10.1093/gji/ggt227.

Davidson PA. 2013b. Turbulence in rotating, stratified and electrically conducting fluids. Cambridge University Press. Online ISBN 781139208673 DOI: https://doi.org/10.1017/CBO9781139208673.

Dormy E, Soward AM. 2007. *Mathematical Aspects of Natural Dynamos*. New York: CRC Press, Taylor and Francis Group. Online ISBN: 9780429145643. https://doi.org/10.1201/9781420055269.

Duka B, Peqini K, De Santis A, Francisco-Carrasco JP. 2015. Using domino model to study the secular variation of the geomagnetic dipolar moment. *Physics of Earth and Planetary Interiors*, **242**: 9-23.http://dx.doi.org/10.1016/j.pepi.2015.03.001.

Gubbins D. 1988. *Mechanism for geomagnetic polarity reversals*. Nature, **335**: 525–528. 10.1038/326167a0

Gubbins D. 1999. The distinction between geomagnetic excursions and reversals. *Geophysical Journal International*, **137(1):** F1–F4. https://doi.org/10.1046/j.1365-246x.1999.00810.x

Guyodo Y, Valet JP. 1999. Global changes in intensity of the Earth's magnetic field during the past 800 kyr. *Nature,* **399**: 249–252. https://doi.org/10.1038/20420.

Guyodo Y, Valet JP. 2006. A comparison of relative paleointensity records of the Matuyama Chron for the period 0.75-1.25 Ma. *Physics of the Earth and Planetary Interiors*, **156 (3-4):** 205–212. https://doi.org/10.1016/j.pepi.2005.03.020.

Hollerbach R, Jones CA. 1993. Influence of the Earth's inner core on geomagnetic fluctuations and reversals. *Nature*, **365**: 541–543. https://doi.org/10.1038/365541a0.

Hollerbach R, Jones CA. 1995. On the magnetically stabilizing role of the Earth's inner core. *Physics of the Earth and Planetary Interiors*, **87 (3-4):** 171–181. https://doi.org/10.1016/0031-9201(94)02965-E.

Hoyng P, Schmitt D, Ossendrijver M. 2002. A theoretical analysis of the observed variability of the geomagnetic dipole field. *Physics of the Earth and Planetary Interiors*, **130**: 143–157. https://doi.org/10.1016/S0031-9201(02)00004-3.

Kageyama A, Sato T. 1997. Velocity and magnetic field structures in a magnetohydrodynamic dynamo. *Physics of Plasmas*, **4 (5):** 1569–1575. https://doi.org/10.1063/1.872287.

McMillan DG, Constable CG. 2006. Limitations in correlation of regional relative geomagnetic paleointensity. *Geochemistry, Geophysics, Geosystems*, **7 (9):** Q09009. https://doi.org/10.1029/2006GC001350.

Merrill RT, McElhinny MW, McFadden PL. 1996. The magnetic field of the Earth: Paleomagnetism, the core, and the deep mantle. International geophysics series. Volume **63**. Academic Press, San Diego. ISBN: 0-12-491246-X.

Molina-Cardín A, Dinis L, Osete ML. 2021. Simple stochastic model for geomagnetic excursions and reversals reproduces the temporal asymmetry of the axial dipole moment. *Earth, Atmospheric, and Planetary Sciences*, **118(10)**: E2017696118**.** https://doi.org/10.1073/pnas.2017696118.

Mori N, Schmitt D, Wicht J, Ferriz-Mas A, Mouri H, Nakamichi A, and Morikawa M. 2013. Domino model for geomagnetic field reversals. *Physical Review E* **87**: 012108. DOI: https://doi.org/10.1103/PhysRevE.87.012108.

Morzfeld M, Buffett BA. 2019. A comprehensive model for the kyr and Myr timescales of Earth's axial magnetic dipole field. *Nonlinear Processes in Geophysics*, **26 (3)**: 123–142. https://doi.org/10.5194/npg-26-123-2019.

Olson P, Amit H. 2014. *Mantle superplumes induce geomagnetic superchrons*. Frontiers in Earth Science, **2**, 22. https://doi.org/10.3389/feart.2015.00038.

Olson PL, Coe RS, Driscoll PE, Glatzmaier GA, Roberts PH, 2010. Geodynamo reversal frequency and heterogeneous core-mantle boundary heat flow. *Physics of Earth and Planetary Interiors*, **180 (1-2):** 66–79. 10.1016/j.pepi.2010.02.010.

Panovska S, Korte M, Finlay CC, Constable CG. 2015. Limitations in paleomagnetic data and modelling techniques and their impact on Holocene geomagnetic field models. *Geophysical Journal International*, **202 (1):** 402–418. https://doi.org/10.1093/gji/ggv137.

Peqini K, Duka B, De Santis A. 2015. Insights into pre-reversal paleosecular variation from stochastic models. *Frontiers in Earth Science*, **3 (52):** 1-13. https://doi.org/10.3389/feart.2015.00052.

Peqini K, Koçi E, Prenga D, Osmanaj R. 2023. The core-mantle boundary velocity field in the recent decades. *AIP Conference Proceedings*, **2872**: 120063. https://doi.org/10.1063/5.0162927.

Peqini K. 2024. Inertial forces reproduce the observed variations of the frequency of geomagnetic reversals. *Albanian Journal of Natural and Technical Sciences* (AJNTS), **61 (2):**3-18. https://akad.gov.al/wp-content/uploads/2025/06/1-Peqini-K.-Inertial-forces-reproduce-the-observed-variations-_Albanian-Journal-of-Natural-and-Technical-Sciences-20242-XXIX-61.pdf.

Schmitt DM, Ossendrijver MAJH, Hoyng P. 2001. Magnetic field reversals and secular variation in a bistable geodynamo model. *Physics of the Earth and Planetary Interiors*, **125 (1-4):** 119–124. https://doi.org/10.1016/S0031-9201(01)00237-0.

Singer BS, Jicha BR, Mochizuki N, Coe RS. 2019. Synchronizing volcanic, sedimentary, and ice core records of Earth's last magnetic polarity reversal. *Science Advances*, **5 (8):** eaaw4621. doi: 10.1126/sciadv.aaw4621.

Valet JP, Fournier A. 2016. Deciphering records of geomagnetic reversals. *Reviews of geophysics*, **54 (2)**: 410–446. https://doi.org/10.1002/2015RG000506.

Valet JP, Meynadier L. 1993. Geomagnetic field intensity and reversals during the past four million years. *Nature*, **366**: 234–238. 10.1038/366234a0.

Valet JP, Meynadier M, Guyodo Y. 2005. Geomagnetic dipole strength and reversal rate over the past two million years. *Nature*, **435**:802–805. doi: 10.1038/nature03674.

Wicht J, Meduri D. 2016. A Gaussian model for simulated geomagnetic field reversals. Physics of the Earth and Planetary Interiors. **259**: 45–60. https://doi.org/10.1016/j.pepi.2016.07.007.

Ziegler LB, Constable CG. 2011. Asymmetry in growth and decay of the geomagnetic dipole. Earth and Planetary Science Letters, **312 (3–4):** 300-304. https://doi.org/10.1016/j.epsl.2011.10.019.